

GAMMA RAYS FROM THERMAL-NEUTRON CAPTURE IN NATURAL AND ^{39}K ENRICHED POTASSIUM

A. M. F. OP DEN KAMP and A. M. J. SPITS

Fysisch Laboratorium, Rijksuniversiteit, Utrecht, Netherlands

Received 20 August 1971

Abstract: Gamma rays following thermal-neutron capture in natural and in ^{39}K enriched potassium have been investigated with a Ge(Li) and a Ge(Li)-NaI spectrometer. In the $^{39}\text{K}(n, \gamma)^{40}\text{K}$ reaction 222 γ -rays were found, of which 187 could be fitted into the level scheme of ^{40}K . Fifteen γ -rays could be ascribed to the $^{41}\text{K}(n, \gamma)^{42}\text{K}$ reaction. Excitation energies of 54 levels in ^{40}K and of 9 levels in ^{42}K have been determined with 0.2–1.0 keV errors. The Q -values of the $^{39}\text{K}(n, \gamma)^{40}\text{K}$ and $^{41}\text{K}(n, \gamma)^{42}\text{K}$ reactions are $Q = 7799.7 \pm 0.8$ keV and 7533.9 ± 1.2 keV, respectively.

E

NUCLEAR REACTIONS $^{39,41}\text{K}$, ^1H , ^6Li , ^{12}C , ^{19}F , ^{40}Ar , ^{56}Fe , $^{207}\text{Pb}(n, \gamma)$, $E =$ thermal; ^{19}F , $^{28}\text{Si}(n, n'\gamma)$, $E =$ fast; measured E_γ , I_γ . K , $^{39}\text{K}(n, \gamma)$, $E =$ thermal; measured E_γ , I_γ , $\gamma\gamma$ -coin; deduced Q . $^{40,42}\text{K}$ deduced levels, γ -branching. Ge(Li), NaI detectors.

1. Introduction

Gamma rays following thermal-neutron capture in natural potassium have been studied with scintillation spectrometers ^{1,2}), magnetic pair spectrometers ^{3,4}) and magnetic Compton spectrometers ^{5,6}). The resolution of these spectrometers is insufficient for an adequate study of the complex $^{39}\text{K}(n, \gamma)^{40}\text{K}$ γ -ray spectrum.

In 1966, Kennett *et al.* ⁷) investigated the $^{39}\text{K}(n, \gamma)^{40}\text{K}$ reaction with a Ge(Li) detector and examined a possible correlation between (n, γ) and (d, p) strengths. This investigation was incomplete because practically only primary γ -rays were studied. A preliminary decay scheme for ^{40}K was obtained by Skeppstedt ⁸) with a three-crystal Ge(Li) pair spectrometer, but this investigation did not give more information than given by Kennett *et al.* ⁷).

To obtain a more detailed picture of the $^{39}\text{K}(n, \gamma)^{40}\text{K}$ reaction the present investigation was performed with high-resolution Ge(Li) spectrometers. The results will be compared with those of Johnson and Kennett ⁹), who recently reported very similar data: 252 γ -ray transitions and 55 excitation energies. Branching ratios of bound states and intensity balances for the deduced levels were not reported.

Excitation energies of ^{40}K levels and I_n values, obtained from the $^{39}\text{K}(d, p)^{40}\text{K}$ reaction, are summarized by Endt and Van der Leun ¹¹). A partial decay scheme and some excitation energies have been deduced by Freeman and Gallman ¹²) from the $^{39}\text{K}(d, p\gamma)^{40}\text{K}$ reaction. Spins for several levels have been determined by Twin

*et al.*¹³⁾ from the $^{40}\text{Ar}(\text{d}, \text{n}\gamma)^{40}\text{K}$ reaction. They also pointed out that the 2290 keV level must be a doublet. The excitation energies of the components are determined in the present investigation.

The natural abundances of ^{39}K , ^{40}K and ^{41}K are 93.1 %, 0.012 % and 6.9 % [ref. ¹¹⁾], their thermal-neutron capture cross sections 1.94 ± 0.15 b, 70 ± 20 b and 1.24 ± 0.10 b [ref. ¹⁴⁾], respectively. About 5 % of the thermal-neutron capture thus will occur in ^{41}K ; the contribution of ^{40}K is negligible. The use of a sample enriched in ^{39}K has helped to differentiate between the $^{39}\text{K}(\text{n}, \gamma)$ and $^{41}\text{K}(\text{n}, \gamma)$ reactions.

2. Experimental

The experiment has been performed at the High Flux Reactor at Petten, Netherlands. The target was placed in a beam of thermal neutrons with a flux of about $10^7 \text{ cm}^{-2} \cdot \text{s}^{-1}$.

The samples used were 400 mg of natural K_2CO_3 and 400 mg K_2CO_3 enriched to 98.3 % in ^{39}K . The enriched sample was on loan from AERE, Harwell, England. The samples were encapsulated in thin-walled teflon tubes. A detailed description of the experimental set-up has been given by van Middelkoop and Spilling¹⁵⁾.

To facilitate the interpretation of a peak as a full-energy, single- or double-escape peak, the γ -rays were detected with true-coaxial Ge(Li) detectors of different volume: 6.5 and 20 cm^3 . The resolution for the 1.33 MeV ^{60}Co γ -ray was 3.0 and 2.6 keV, respectively. The overall resolution (measuring time 4 d) of the system with the 20 cm^3 Ge(Li) detector was 2.9 keV at $E_\gamma = 1.27$ MeV and 5.9 keV at $E_\gamma = 6.7$ MeV.

Gamma rays from the $^{12}\text{C}(\text{n}, \gamma)^{13}\text{C}$ and $^{56}\text{Fe}(\text{n}, \gamma)^{57}\text{Fe}$ reactions and from radioactive sources (table 1) together with the γ -rays from the $^{39}\text{K}(\text{n}, \gamma)^{40}\text{K}$ reaction were investigated with a 23 cm^3 Ge(Li) detector to obtain an accurate energy calibration. The resolution of this detector was 3.0 keV for the 1.33 MeV ^{60}Co γ -ray. The linearity of the system with the 23 cm^3 detector was tested with a precision pulse generator.

Various runs, covering the $E_\gamma = 0.1$ –2.5 and 0.5–0.7 MeV regions were made with the different detectors. Separate runs covering the same energy regions were performed to investigate the background radiation. Gamma rays from the enriched sample were only measured with the 20 cm^3 Ge(Li) detector. The electronic equipment consisted of an Ortec FET preamplifier, an Ortec main amplifier and a Laben 4096-channel pulse-height analyser.

Gamma-gamma coincidence measurements were performed with a sample of 7 g natural potassium. The coincidence set-up consisted of the 20 cm^3 Ge(Li) detector and a 12.7 cm \times 12.7 cm NaI crystal. The time resolution of the coincidence system was $2\tau = 80$ ns. A digital discriminator¹⁶⁾ with 16 windows routed the subgroups of the memory. Thirteen windows were placed on the pulse-height spectrum of the Ge(Li) detector. About 1 % of the incoming pulses passed the discriminator; 5 % of the accepted pulses was due to random events. The counting rate after the discriminator was 3.8 s^{-1} . The total measuring time was 39 d.

3. Analysis of the measurements

The energy calibration for each spectrum was obtained by fitting a sixth-degree polynomial to the calibration lines (see below). The γ -ray spectra measured with the 23 cm³ Ge(Li) detector were analysed to obtain an accurate set of internal calibration energies.

The positions of the peaks were determined by fitting Gaussian functions to the experimental points.

TABLE 1
Energies of γ -rays used for calibration

Isotope ^{a)}	E_γ (keV) ^{b)}	Ref.	Isotope ^{a)}	E_γ (keV) ^{b)}	Ref.
⁵⁷ Co (r)	122.05 ± 0.05	¹⁷⁾	²² Na (r)	1274.52 ± 0.07	²⁰⁾
¹⁹ F	197.2 ± 0.2	¹⁸⁾	⁶⁰ Co (r)	1332.48 ± 0.05	¹⁷⁾
annihilation	511.01 ± 0.01	¹⁷⁾	²⁰ Ne	1633.4 ± 0.3	¹⁸⁾
²⁰ F	583.5 ± 0.3	¹⁸⁾	⁸⁸ Y (r)	1836.08 ± 0.08	²⁰⁾
¹³⁷ Cs (r)	611.59 ± 0.08	¹⁹⁾	² H	2223.35 ± 0.05	²¹⁾
⁵⁴ Mn (r)	834.84 ± 0.08	²⁰⁾	¹³ C	4945.0 ± 0.2	¹⁸⁾
⁸⁸ Y (r)	898.01 ± 0.08	²⁰⁾	⁵⁷ Fe	7631.0 ± 0.5	¹⁸⁾
⁶⁰ Co (r)	1173.23 ± 0.04	¹⁷⁾	⁵⁷ Fe	7645.2 ± 0.5	¹⁸⁾

^{a)} The symbol (r) denotes radioactive source. The ²H, ¹³C, ²⁰F and ⁵⁷Fe γ -rays originate from thermal-neutron capture in ¹H, ¹²C, ¹⁹F and ⁵⁶Fe, respectively, the ¹⁹F and ²⁰Ne γ -rays from the ¹⁹F(n, n' γ) and ¹⁹F(n, γ)²⁰F(β^-)²⁰Ne reactions, respectively.

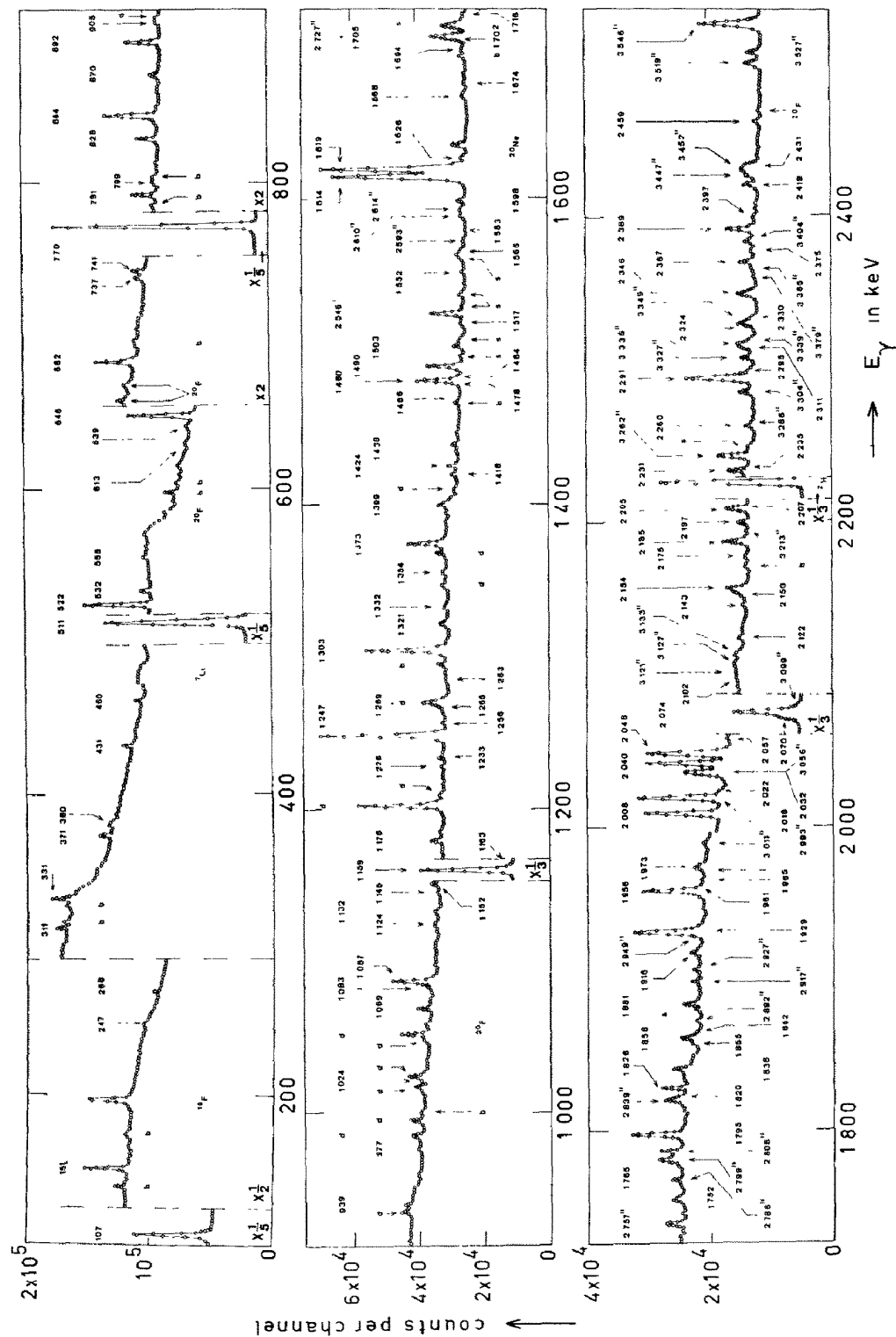
^{b)} Uncorrected for recoil.

The low-energy spectrum ($E_\gamma = 0.1$ –2.5 MeV) was calibrated with the lines listed in table 1. The calibration curve deviates at most $\Delta E = 0.2$ keV from a linear fit. The standard deviation between the energies calculated from the calibration curve, and the calibration energy was $\sigma = 0.06$ keV. The energies of some prominent γ -rays thus obtained together with the ¹²C(n, γ)¹³C and ⁵⁶Fe(n, γ)⁵⁷Fe energies listed in table 1, were used for the energy calibration of the high-energy spectrum ($E_\gamma = 0.5$ –7.0 MeV). Moreover, 52 energy relations in the form of 511 or 1022 keV differences between full-energy peaks and escape peaks were used as constraints in the least-squares fitting problem, leading to $\Delta E = 0.7$ keV and $\sigma = 0.2$ keV.

The spectra measured with the 20 cm³ Ge(Li) detector were analysed to resolve complex parts and to determine the intensities of all γ -lines precisely.

Peak positions were determined from a least-squares fitting of a slightly asymmetric response function to the observed peaks. Isolated peaks were used to determine the asymmetry and the FWHM as a function of energy. The program allowed the analysis of a group of up to six overlapping peaks. With this detector one finds $\Delta E = 0.4$ and 0.3 keV and $\sigma = 0.06$ and 0.2 keV for the energy calibration of the low- and high-energy spectra, respectively.

Intensities were calculated by means of efficiency curves for full-energy, single- and double-escape peaks. These curves were determined as described in ref. ²³⁾.



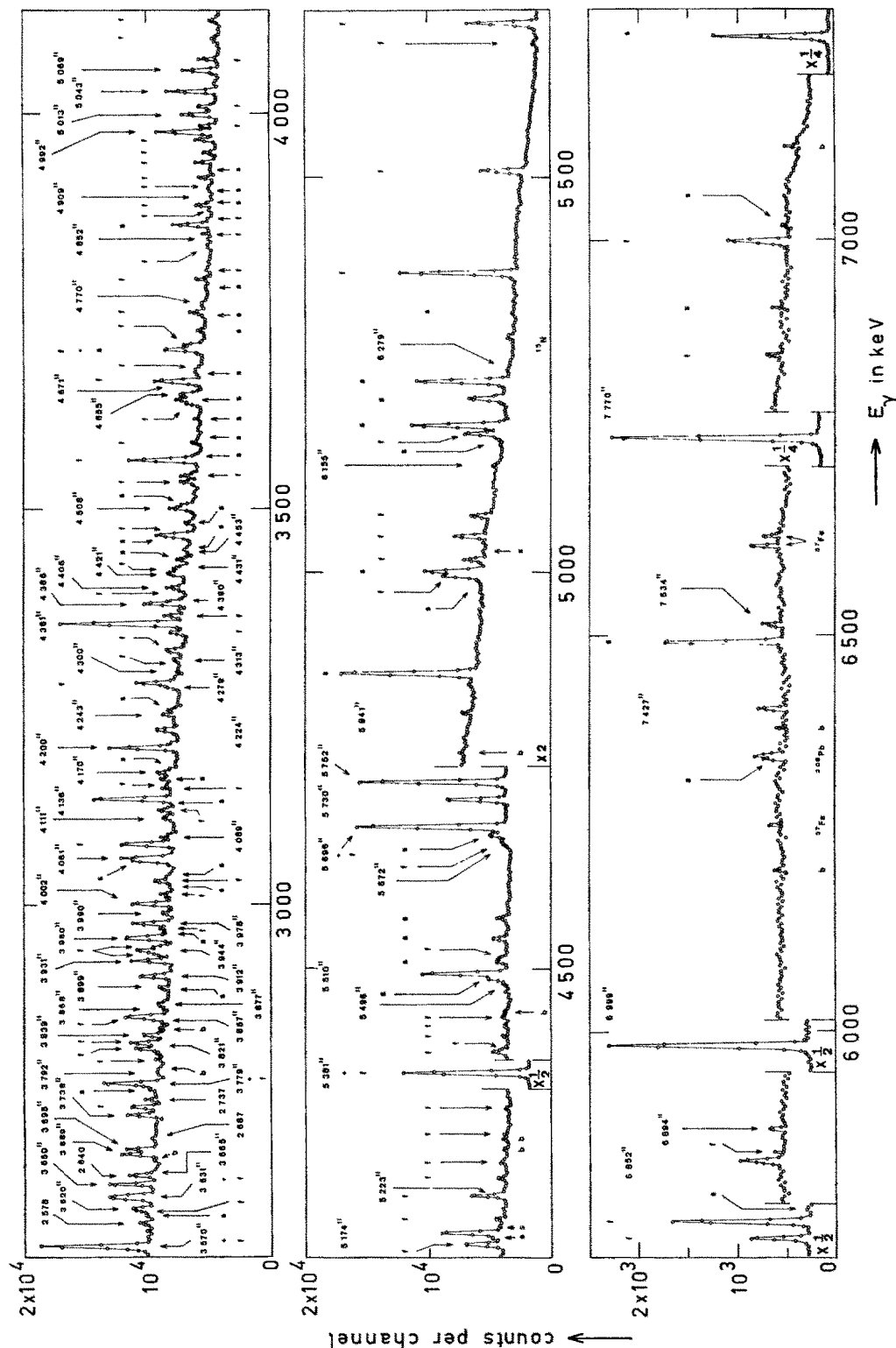


Fig. 2. The high-energy $^{39}\text{K}(n,\gamma)^{40}\text{K}$ spectrum measured with the 20 cm³ Ge(Li) detector. Gamma-ray energies are indicated (in keV) at the double-escape peaks. Other peaks are labelled f or s, according to their full-energy or single-energy character, respectively. The background has been subtracted (see text). In smooth regions in between peaks the mean of each three consecutive points is plotted.

TABLE 2
Observed γ -rays from the $^{39}\text{K}(n, \gamma)^{40}\text{K}$ reaction

$E_\gamma + E_x$ ^{a)} (keV)	Intensity ^{b)}	Interpretation (E_x in keV) ^{c)}	$E_\gamma + E_x$ ^{a)} (keV)	Intensity ^{b)}	Interpretation (E_x in keV) ^{c)}
246.9 \pm 0.3	0.16 \pm 0.02	4149 \rightarrow 3902 (4396 \rightarrow 4149) (3394 \rightarrow 3146)	1354.3 \pm 0.2	0.45 \pm 0.06	4465 \rightarrow 3110
			1373.1 \pm 0.2	1.78 \pm 0.07	3664 \rightarrow 2291
			1398.8 \pm 0.2	0.27 \pm 0.04	2291 \rightarrow 892
310.7 \pm 0.2	0.16 \pm 0.02	3797 \rightarrow 3487	1418.2 \pm 0.2	0.21 \pm 0.10	4149 \rightarrow 2731
330.5 \pm 0.2	0.49 \pm 0.04	2290 \rightarrow 1959	1424.3 \pm 0.2	0.45 \pm 0.04	3822 \rightarrow 2397
371.4 \pm 0.2	0.23 \pm 0.03	3128 \rightarrow 2756 (2419 \rightarrow 2047) (4908 \rightarrow 4537)	1438.4 \pm 0.3	0.35 \pm 0.04	4807 \rightarrow 3368
			1466.1 \pm 0.3	0.31 \pm 0.06	3110 \rightarrow 1644
			1477.5 \pm 0.3	0.28 \pm 0.05	3738 \rightarrow 2261
380.2 \pm 0.3	0.18 \pm 0.02	3110 \rightarrow 2731	1479.9 \pm 0.2	2.28 \pm 0.09	3439 \rightarrow 1959
459.6 \pm 0.2	0.25 \pm 0.03	2419 \rightarrow 1959	1483.9 \pm 0.4	0.14 \pm 0.02	3128 \rightarrow 1644
522.2 \pm 1.0	2.0 \pm 0.9	2626 \rightarrow 2104	1489.6 \pm 0.2	1.81 \pm 0.08	2290 \rightarrow 800
554.9 \pm 0.2	0.18 \pm 0.02	3923 \rightarrow 3368	1502.8 \pm 0.4	0.51 \pm 0.18	3146 \rightarrow 1644
612.8 \pm 0.3	0.13 \pm 0.03	3599 \rightarrow 2986	1517.0 \pm 0.3	0.23 \pm 0.03	4465 \rightarrow 2947
646.2 \pm 0.1	2.86 \pm 0.09	2290 \rightarrow 1644	1551.5 \pm 0.3	0.23 \pm 0.03	3599 \rightarrow 2047
736.8 \pm 0.2	0.24 \pm 0.03	4105 \rightarrow 3368	1565.6 \pm 0.4	0.25 \pm 0.04	
741.0 \pm 0.2	0.32 \pm 0.03	3869 \rightarrow 3128	1582.9 \pm 0.6	0.09 \pm 0.02	3630 \rightarrow 2047
770.4 \pm 0.1	56.1 \pm 1.2	800 \rightarrow 30	1597.8 \pm 0.3	0.35 \pm 0.03	3888 \rightarrow 2290
791.2 \pm 0.2	0.68 \pm 0.03	3599 \rightarrow 2808			(4744 \rightarrow 3146)
799.4 \pm 0.2	0.16 \pm 0.02	4537 \rightarrow 3738	1613.7 \pm 0.2	7.62 \pm 0.19	1644 \rightarrow 30
827.7 \pm 0.3	0.60 \pm 0.04	2787 \rightarrow 1959	1618.9 \pm 0.2	8.2 \pm 0.2	2419 \rightarrow 800
843.6 \pm 0.2	1.50 \pm 0.18	1644 \rightarrow 800	1625.5 \pm 0.3	0.32 \pm 0.04	
870.2 \pm 0.3	0.28 \pm 0.06		1667.6 \pm 0.6	0.22 \pm 0.07	3738 \rightarrow 2070
891.6 \pm 0.2	1.16 \pm 0.05	892 \rightarrow 0	1674.1 \pm 0.4	0.18 \pm 0.04	
904.5 \pm 0.3	0.15 \pm 0.03	4807 \rightarrow 3902	1694.0 \pm 0.6	0.26 \pm 0.06	3797 \rightarrow 2104
939.1 \pm 0.2	0.24 \pm 0.03	2986 \rightarrow 2047	1702.0 \pm 0.4	0.53 \pm 0.08	
977.1 \pm 0.3	0.21 \pm 0.03	4105 \rightarrow 3128	1704.6 \pm 0.3	1.85 \pm 0.10	3664 \rightarrow 1959
1023.8 \pm 0.3	0.39 \pm 0.07	3128 \rightarrow 2104 (3599 \rightarrow 2575)	1718.1 \pm 0.6	0.27 \pm 0.08	3822 \rightarrow 2104 (4666 \rightarrow 2947)
1069.1 \pm 0.2	0.38 \pm 0.03	4807 \rightarrow 3738	1752.0 \pm 0.3	0.40 \pm 0.04	3711 \rightarrow 1959
1083.1 \pm 0.3	0.24 \pm 0.04	3840 \rightarrow 2756	1765.0 \pm 0.3	0.30 \pm 0.03	3869 \rightarrow 2104
1086.9 \pm 0.2	1.43 \pm 0.06	2731 \rightarrow 1644	1795.3 \pm 0.3	1.84 \pm 0.06	3439 \rightarrow 1644
1123.9 \pm 0.3	0.26 \pm 0.26	3414 \rightarrow 2290	1819.5 \pm 0.5	0.34 \pm 0.10	3923 \rightarrow 2104
1131.6 \pm 0.3	0.32 \pm 0.04	3888 \rightarrow 2751	1825.7 \pm 0.3	0.83 \pm 0.06	2626 \rightarrow 800
1144.9 \pm 0.4	0.17 \pm 0.04	4744 \rightarrow 3599	1838.3 \pm 0.3	0.51 \pm 0.04	3797 \rightarrow 1959
1151.8 \pm 0.3	0.33 \pm 0.06	3110 \rightarrow 1959			(4465 \rightarrow 2626)
1159.0 \pm 0.1	10.0 \pm 0.3	1959 \rightarrow 800	1854.5 \pm 0.4	0.30 \pm 0.07	3902 \rightarrow 2047
1162.8 \pm 0.3	0.50 \pm 0.06	3738 \rightarrow 2575 (4149 \rightarrow 2986)	1858.2 \pm 0.3	0.76 \pm 0.05	4149 \rightarrow 2291 (4666 \rightarrow 2808)
1178.3 \pm 0.2	0.37 \pm 0.03	2070 \rightarrow 892	1881.1 \pm 0.3	0.63 \pm 0.05	3840 \rightarrow 1959 (4908 \rightarrow 3027)
1226.1 \pm 0.3	0.12 \pm 0.02	3487 \rightarrow 2261			
1233.0 \pm 0.3	0.19 \pm 0.03	3630 \rightarrow 2397	1915.9 \pm 0.3	0.42 \pm 0.04	4020 \rightarrow 2104
1247.2 \pm 0.2	4.89 \pm 0.12	2047 \rightarrow 800	1929.2 \pm 0.2	2.85 \pm 0.12	1959 \rightarrow 30
1256.0 \pm 0.5	0.13 \pm 0.05		1956.5 \pm 0.2	2.55 \pm 0.10	2756 \rightarrow 800
1266.1 \pm 0.3	0.38 \pm 0.05	3664 \rightarrow 2397	1961.2 \pm 0.6	0.14 \pm 0.03	4587 \rightarrow 2626
1269.2 \pm 0.2	0.36 \pm 0.10	2070 \rightarrow 800	1964.5 \pm 0.6	0.14 \pm 0.03	3923 \rightarrow 1959
1283.1 \pm 0.3	0.20 \pm 0.03				(4254 \rightarrow 2290)
1303.4 \pm 0.2	3.50 \pm 0.10	2104 \rightarrow 800	1972.9 \pm 0.3	0.45 \pm 0.06	4020 \rightarrow 2047
1320.9 \pm 0.3	0.36 \pm 0.05	3368 \rightarrow 2047	2007.6 \pm 0.3	3.18 \pm 0.10	2808 \rightarrow 800
1331.9 \pm 0.3	0.29 \pm 0.04		2017.6 \pm 0.3	3.8 \pm 0.2	2047 \rightarrow 30

TABLE 2 (continued)

$E_\gamma + E_r$ ^{a)} (keV)	Intensity ^{b)}	Interpretation (E_x in keV) ^{c)}	$E_\gamma + E_r$ ^{a)} (keV)	Intensity ^{b)}	Interpretation (E_x in keV) ^{c)}
2022.3±0.6	0.22±0.04		2949.3±0.8	0.54±0.06	4908 → 1959
2032.1±0.5	0.60±0.14	4789 → 2756	2992.5±0.7	0.61±0.11	C → 4807
2040.1±0.3	3.5 ±0.2	2070 → 30	3010.6±0.6	0.77±0.18	C → 4789
2047.5±0.3	3.60±0.14	2047 → 0	3055.6±0.4	2.8 ±0.2	C → 4744
2057.2±0.6	0.23±0.05	4105 → 2047	3099.3±0.6	1.11±0.16	4744 → 1644
2069.7±0.3	2.16±0.14	2070 → 0	3120.5±0.7	0.28±0.07	
2073.7±0.3	8.7 ±0.5	2104 → 30	3127.0±0.5	0.61±0.10	3128 → 0
2102.1±0.9	0.10±0.03	4149 → 2047	3133.0±0.7	0.40±0.11	C → 4666
2122.2±0.5	0.27±0.03	4908 → 2787	3213.4±0.9	0.26±0.06	C → 4587
2143.3±0.4	0.23±0.03		3262.2±0.4	2.8 ±0.2	C → 4537
2150.1±0.4	0.65±0.05	4254 → 2104	3285.8±1.2	0.25±0.07	
2153.8±0.3	0.95±0.04	3797 → 1644	3304.0±0.5	1.11±0.16	4105 → 800
2175.0±0.5	0.19±0.02	4465 → 2290	3326.8±0.5	0.93±0.19	
2184.5±0.4	1.20±0.07	4254 → 2070	3336.0±0.5	1.27±0.11	C → 4465
2196.9±0.4	0.60±0.05	3840 → 1644	3339.1±0.6	0.60±0.11	3368 → 30
2205.1±0.6	0.61±0.20		3349.0±0.4	1.3 ±0.3	4149 → 800
2206.9±0.6	0.9 ±0.2	4254 → 2047	3379.3±0.7	0.30±0.08	
2230.7±0.3	1.29±0.15	2261 → 30	3384.5±1.1	0.42±0.10	3414 → 30
2234.5±0.9	0.16±0.05		3403.6±0.5	1.08±0.19	C → 4396
2260.4±0.4	0.43±0.05	2261 → 0	3447.0±0.5	0.75±0.18	
2290.7±0.3	3.60±0.14	2291 → 0	3453.6±1.0	1.5 ±0.7	4254 → 800
2294.9±0.6	0.48±0.06	4254 → 1959	3518.9±0.5	1.06±0.13	
2310.5±0.5	0.66±0.08	3110 → 800	3526.9±0.4	1.00±0.13	
2324.3±0.8	0.21±0.06	4744 → 2419	3545.8±0.4	4.5 ±0.4	C → 4254
2330.4±0.5	0.43±0.06		3569.8±0.9	0.50±0.08	3599 → 30
2346.0±0.7	0.99±0.10	3146 → 800	3619.7±0.5	0.84±0.13	
2367.4±0.4	1.9 ±0.3	2397 → 30	3630.7±0.6	0.50±0.03	3630 → 0
2374.8±0.5	0.40±0.05	4666 → 2291	3650.4±0.4	2.6 ±0.4	C → 4149
2389.3±0.3	1.89±0.19	2419 → 30	3664.7±1.6	0.40±0.17	4465 → 800
2397.1±0.5	0.34±0.05	2397 → 0	3688.9±0.4	1.44±0.18	
2418.6±0.5	0.83±0.08	2419 → 0	3695.3±0.4	1.32±0.17	C → 4105
2430.5±0.4	0.81±0.11		3737.5±0.6	1.3 ±0.3	4537 → 800
2459.3±1.6	0.23±0.12		3779.3±0.6	0.88±0.19	C → 4020
2546.2±0.6	3.0 ±0.7	2575 → 30	3791.9±1.2	0.25±0.08	3822 → 30
2577.6±0.6	0.48±0.07	4537 → 1959	3821.4±0.7	0.47±0.04	3822 → 0
2593.4±1.2	0.49±0.13	3394 → 800	3838.5±0.5	0.69±0.18	3869 → 30
2609.9±0.4	1.1 ±0.2	4254 → 1644	3857.5±0.8	0.47±0.12	3888 → 30
2614.0±0.4	1.55±0.16	3414 → 800	3868.2±1.3	0.21±0.06	3869 → 0
2639.6±0.7	1.05±0.17	3439 → 800	3877.0±0.8	0.50±0.11	C → 3923
2686.8±0.7	0.28±0.05	3487 → 800	3898.5±1.3	0.37±0.17	C → 3902
2726.6±0.4	1.25±0.13	2756 → 30	3911.9±0.5	1.2 ±0.3	C → 3888
2736.6±0.9	0.56±0.14	4807 → 2070	3930.8±0.5	1.51±0.18	C → 3869
2756.7±0.4	1.7 ±0.2	2787 → 30	3944.0±0.5	1.00±0.17	4744 → 800
2786.1±1.0	0.33±0.09	2787 → 0	3959.6±0.5	1.6 ±0.3	C → 3840
2799.1±0.4	1.28±0.19	3599 → 800	3978.1±0.5	1.4 ±0.2	C → 3822
2806.1±0.4	1.70±0.17		3989.5±0.8	0.45±0.08	4789 → 800
2839.1±0.4	1.7 ±0.3	4908 → 2070	4001.9±0.5	1.7 ±0.2	C → 3797
2892.1±0.6	0.36±0.07	C → 4908	4061.4±0.6	1.8 ±0.3	C → 3738
2917.4±0.4	0.67±0.11	2947 → 30	4088.8±0.7	0.51±0.17	C → 3711
2926.8±0.4	0.65±0.11		4110.7±0.8	0.63±0.15	

TABLE 2 (continued)

$E_\gamma + E_r$ ^{a)} (keV)	Intensity ^{b)}	Interpretation (E_x in keV) ^{c)}	$E_\gamma + E_r$ ^{a)} (keV)	Intensity ^{b)}	Interpretation (E_x in keV) ^{c)}
4136.0 \pm 0.5	3.4 \pm 0.4	C \rightarrow 3664	4769.5 \pm 1.2	0.38 \pm 0.12	
4169.8 \pm 0.6	0.85 \pm 0.14	C \rightarrow 3630	4851.8 \pm 1.0	0.18 \pm 0.04	C \rightarrow 2947
4200.3 \pm 0.5	2.5 \pm 0.3	C \rightarrow 3599	4908.6 \pm 1.3	0.10 \pm 0.04	4908 \rightarrow 0
4224.1 \pm 0.6	0.84 \pm 0.13	4254 \rightarrow 30	4992.0 \pm 0.6	2.5 \pm 0.4	C \rightarrow 2808
4243.0 \pm 0.7	0.53 \pm 0.10		5013.3 \pm 0.6	1.58 \pm 0.17	C \rightarrow 2787
4279.0 \pm 0.6	0.56 \pm 0.08		5043.2 \pm 0.6	2.4 \pm 0.3	C \rightarrow 2756
4299.9 \pm 1.1	0.24 \pm 0.07		5069.2 \pm 0.6	1.5 \pm 0.3	C \rightarrow 2731
4313.0 \pm 0.7	0.38 \pm 0.06	C \rightarrow 3487	5173.9 \pm 0.6	2.9 \pm 0.3	C \rightarrow 2626
4360.6 \pm 0.5	5.1 \pm 0.5	C \rightarrow 3439	5223.2 \pm 1.4	0.37 \pm 0.11	C \rightarrow 2575
4385.5 \pm 0.5	1.8 \pm 0.3	C \rightarrow 3414	5380.8 \pm 0.6	9.8 \pm 0.9	C \rightarrow 2419
4390.1 \pm 0.8	0.59 \pm 0.16		5495.9 \pm 2.2	0.12 \pm 0.06	
4406.0 \pm 1.3	0.6 \pm 0.3	C \rightarrow 3394	5509.8 \pm 0.7	4.1 \pm 0.4	C \rightarrow 2290
4421.3 \pm 0.6	0.55 \pm 0.09		5696.2 \pm 0.6	7.0 \pm 0.7	C \rightarrow 2104
4431.1 \pm 0.6	0.79 \pm 0.14	C \rightarrow 3368	5730.0 \pm 0.6	3.0 \pm 0.3	C \rightarrow 2070
4452.6 \pm 1.1	0.31 \pm 0.08		5752.4 \pm 0.6	7.1 \pm 0.5	C \rightarrow 2047
4507.9 \pm 0.6	1.0 \pm 0.3	4537 \rightarrow 30	5840.9 \pm 1.0	0.23 \pm 0.08	C \rightarrow 1959
4654.5 \pm 0.8	0.9 \pm 0.3	C \rightarrow 3146	6999.4 \pm 0.8	2.7 \pm 0.3	C \rightarrow 800
4671.4 \pm 1.4	0.6 \pm 0.3	C \rightarrow 3128	7769.6 \pm 0.8	7.3 \pm 0.7	C \rightarrow 30

^{a)} The recoil correction is denoted by E_r .

^{b)} The total intensity of the primary γ -rays has been normalized at 100.

^{c)} Alternative interpretations are given between brackets; C denotes the capturing state.

4. Results

Fig. 1 shows the low-energy γ -ray spectrum; fig. 2 shows the γ -ray spectrum in the energy region from 2.5–7.0 MeV. Both spectra were measured with the 20 cm³ Ge(Li) detector. The background has been subtracted. Peaks originating from incomplete background subtraction or from impurities in the sample are labelled with "b" or the symbol of the final nucleus.

Energies and intensities of γ -rays from thermal-neutron capture in ³⁹K are given in table 2. The values listed are the weighted means of those deduced from full-energy, single-escape and double-escape peaks. All energies are recoil corrected. The errors in the γ -ray energies also contain a systematic part of 100 ppm. It originates from (i) systematic errors in the calibration energies, especially in the high-energy region, (ii) the use of extrapolation methods (energy relations) to calculate the energies for $E_\gamma > 2.5$ MeV and (iii) the use of calibration lines from the ³⁹K(n, γ)⁴⁰K reaction for the energy calibration of the spectra measured with the 20 cm³ Ge(Li) detector.

The intensities of the γ -rays are normalized such that the sum of the primary intensities equals 100. Errors in the intensities given in table 2 contain in addition to the statistical errors the estimated errors in the efficiency curves used; the latter amount to 2 % for $E_\gamma \leq 2$ MeV, and increase up to 10 % at $E_\gamma = 10$ MeV.

Energies and intensities of γ -rays from thermal-neutron capture in ^{41}K are given in table 3. No peaks could be ascribed to γ -rays from capture in ^{40}K .

The decay scheme, the excitation energies of bound states and the reaction energy for the relevant potassium isotopes have been determined with a computer program. First the program determines all possible transitions in the decay scheme by comparing each γ -ray energy with the differences between the excitation energies following from the (d, p) work ¹⁰). The program selects those γ -ray energies which correspond with

TABLE 3
Observed γ -rays from the $^{41}\text{K}(n, \gamma)^{42}\text{K}$ reaction

$E_\gamma + E_r$ ^{a)} (keV)	Intensity ^{b)}	Interpretation ^{c)} (E_r in keV)
107.1 \pm 0.3	58 \pm 2	107 \rightarrow 0
151.4 \pm 0.2	20 \pm 1.4	258 \rightarrow 107 ^{d)}
268.4 \pm 0.3	4.5 \pm 0.5	1113 \rightarrow 845 ^{d)}
431.3 \pm 0.3	4.6 \pm 0.7	1113 \rightarrow 682 ^{d)}
532.0 \pm 2.0	9 \pm 3	639 \rightarrow 107
639.0 \pm 0.3	8.0 \pm 0.9	639 \rightarrow 0
682.0 \pm 0.2	32.0 \pm 1.6	682 \rightarrow 0
1861.9 \pm 0.4	7.0 \pm 0.9	1862 \rightarrow 0
5672.0 \pm 1.1	9 \pm 3	C \rightarrow 1862
6155.2 \pm 0.9	2.8 \pm 1.2	C \rightarrow 1379 ^{d)}
6278.8 \pm 0.7	3.9 \pm 1.2	C \rightarrow 1255 ^{d)}
6851.7 \pm 1.0	10 \pm 4	C \rightarrow 682
6894.2 \pm 1.3	3.4 \pm 1.6	C \rightarrow 639
7427.0 \pm 0.8	5.9 \pm 2	C \rightarrow 107
7533.9 \pm 1.2	3.4 \pm 1.3	C \rightarrow 0

^{a)} The recoil correction is denoted by E_r .

^{b)} Intensity in arbitrary units.

^{c)} The capturing state is denoted by C.

^{d)} Interpretation from ref. ⁸⁾.

only one possible transition, within the limits set by the standard deviations, and which were also accepted in a cascade from the capturing state, via known intermediate levels to the ground state. Secondly, the program selects γ -rays which were observed in the coincidence measurements (table 6) and which could easily be fitted in the decay scheme. Some γ -ray assignments were based on intensities. The energies of the γ -rays which thus were positioned in the decay scheme form an over-determined set of linear equations with the excitation energies and the Q -value as unknowns. Finally, the program repeats the calculations with excitation energies and Q -value which follow from the solution of the least-squares problem mentioned.

The measured excitation energies of ^{40}K levels are compared with published values in table 4. The reaction energy determined as $Q = 7799.7 \pm 0.8$ keV is in agreement with the values reported in ref. ⁹⁾ ($Q = 7800.5 \pm 0.2$ keV; this error does not contain a contribution for the error in the calibration procedure) and ref. ⁸⁾ ($Q = 7798.6 \pm$

TABLE 4
Excitation energies and intensity balances of levels in ^{40}K

present investigation ^{a)}	E_x (keV)		Intensity ^{c)}	
	ref. ^{a)}	refs. ^{11, 12)} ^{b)}	in	out
0	0	0	119.8	
29.8 \pm 0.2	29.6 \pm 1.0	29.6 \pm 0.8	106.3	^{d)}
800.1 \pm 0.2	800.0 \pm 1.0	799.9 \pm 0.8	59.0	56.1
891.6 \pm 0.2	892.0 \pm 1.0	891.6 \pm 0.2	0.6	1.2
1643.7 \pm 0.2	1643.5 \pm 1.0	1644 ^{e)}	10.8	9.1
1959.1 \pm 0.3	1959.2 \pm 1.3	1958.8 \pm 0.9	9.3	12.9
2047.4 \pm 0.3	2047.3 \pm 1.1	2047.1 \pm 1.0	9.9	12.3
2069.7 \pm 0.3	2069.3 \pm 0.8	2069.9 \pm 1.3	6.7	6.4
2103.7 \pm 0.3	2104.3 \pm 1.4	2103.5 \pm 0.9	11.6	12.2
2260.5 \pm 0.3		2256 \pm 8	0.4	1.7
2289.8 \pm 0.3	2290.4 \pm 0.7	2290 \pm 2	4.9	5.2
2290.5 \pm 0.3			3.0	3.1
2397.3 \pm 0.4		2393 \pm 4	1.0	1.3
2419.0 \pm 0.3	2418.8 \pm 0.9	2419 \pm 2	10.0	11.1
	2457.5 \pm 2.0			
	2557.9 \pm 0.9			
2575.3 \pm 0.5	2576.7 \pm 2.0	2569 \pm 8	0.9	3
2625.8 \pm 0.4	2626.5 \pm 2.1	2625.7 \pm 1.0	3.0	2.9
2730.6 \pm 0.4	2730.1 \pm 1.3		1.9	1.4
2756.4 \pm 0.4	2756.2 \pm 1.9	2757 \pm 2	3.8	3.8
2786.6 \pm 0.4	2786.2 \pm 0.9	2787 \pm 2	1.8	2.6
2807.8 \pm 0.4	2807.7 \pm 0.8	2808 \pm 2	3.2	3.2
2947.5 \pm 0.5	2946.5 \pm 1.3	2948 \pm 8	0.4	0.7
2986.4 \pm 0.7	2978.6 \pm 0.8	2988 \pm 8	0.1	0.2
	3027.1 \pm 1.3	3030 \pm 4		
3110.4 \pm 0.4	3109.1 \pm 1.4	3108 \pm 8	0.5	1.5
3127.6 \pm 0.4	3128.3 \pm 1.0	3128 \pm 4	1.2	1.4
3146.2 \pm 0.5	3146.6 \pm 1.3	3146 \pm 5	0.9	1.5
3368.4 \pm 0.4	3367.1 \pm 1.3	3365 \pm 4	1.5	1.0
3393.6 \pm 1.0	3378.3 \pm 2.3	3392 \pm 4	0.6	0.5
3413.9 \pm 0.6	3414.4 \pm 1.8	3414 \pm 3	1.8	2.2
3439.0 \pm 0.5	3438.7 \pm 1.1		5.1	5.1
3486.8 \pm 0.6	3485.7 \pm 1.3	3481 \pm 8	0.5	0.4
3599.1 \pm 0.5	3599.9 \pm 1.3	3599 \pm 2	2.7	2.8
3630.3 \pm 0.6	3630.5 \pm 2.0	3630 \pm 3	0.8	0.8
3663.6 \pm 0.4	3663.6 \pm 0.8	3664 \pm 2	3.4	4.0
3711.1 \pm 0.5	3713.2 \pm 1.3	3714 \pm 5	0.5	0.4
3737.9 \pm 0.4	3738.3 \pm 1.2	3739 \pm 2	2.3	1.0
	3767.6 \pm 0.8	3768 \pm 4		
3797.5 \pm 0.4	3797.2 \pm 1.3	3798 \pm 2	1.7	1.9
3821.6 \pm 0.5	3822.3 \pm 1.1	3822 \pm 2	1.4	1.4
3840.2 \pm 0.5	3839.0 \pm 1.1	3840 \pm 2	1.6	1.5
3868.6 \pm 0.4	3875.0 \pm 0.8	3867 \pm 2	1.5	1.5
3887.8 \pm 0.5	3887.7 \pm 1.3	3886 \pm 2	1.2	1.1
3902.1 \pm 0.5	3897.8 \pm 0.8	3898 \pm 8	0.7	0.3
3923.3 \pm 0.5		3920 \pm 8	0.5	0.7
4020.0 \pm 0.5	4019.8 \pm 1.1	4017 \pm 8	0.9	0.9

TABLE 4 (continued)

present investigation ^{a)}	E_x (keV)		Intensity ^{c)}	
	ref. ⁹⁾	refs. ^{11, 12)} ^{b)}	in	out
4104.6 \pm 0.5	4104.0 \pm 1.0	4102 \pm 8	1.3	1.8
4148.9 \pm 0.5	4149.3 \pm 0.9		2.6	2.5
4253.9 \pm 0.5	4253.6 \pm 0.6	4253 \pm 8	4.5	6.7
	4273.3 \pm 1.5			
	4281.1 \pm 1.1			
4396.1 \pm 0.7	4397.2 \pm 1.2	4396 \pm 8	1.1	
4464.6 \pm 0.5	4462.8 \pm 1.2	4462 \pm 8	1.3	1.3
4537.3 \pm 0.5	4537.8 \pm 0.7	4539 \pm 8	2.8	2.9
4586.8 \pm 0.8	4579.6 \pm 1.0	4582 \pm 8	0.3	0.1
4665.8 \pm 0.7		4658 \pm 8	0.4	0.4
4743.9 \pm 0.5	4744.7 \pm 1.9		2.8	2.5
4788.9 \pm 0.7	4792.7 \pm 1.4	4788 \pm 8	0.8	1.0
4806.9 \pm 0.5	4808.5 \pm 0.9	4801 \pm 8	0.6	1.4
4908.5 \pm 0.6	4908.6 \pm 0.9	4902 \pm 8	0.4	2.6
7799.7 \pm 0.8 ^{f)}	7800.5 \pm 0.2 ^{f)}	7801.5 \pm 2.7 ^{f)}		100

^{a)} The results are obtained from least-squares analysis. The errors have been enlarged with 100 ppm to incorporate a possible systematic error.

^{b)} Excitation energies with a deviation less than 2 keV are from ref. ¹²⁾; all other excitation energies are from ref. ¹¹⁾.

^{c)} The total intensity of the primary γ -rays has been normalized at 100.

^{d)} Not observed (see text).

^{e)} No error given.

^{f)} Reaction Q -value.

1.0 keV). The value reported in the 1965 mass table ²²⁾ is $Q = 7801.5 \pm 2.7$ keV. Some excitation energies in ^{42}K and the $^{41}\text{K}(n, \gamma)^{42}\text{K}$ reaction energy are given in table 5.

The decay schemes of ^{40}K and ^{42}K are shown in figs. 3 and 4, respectively. The excitation energies, the intensities of the primary γ -rays and the branching ratios for the bound states are from the present investigation. The $I_n(d, p)$ values for levels in ^{40}K and ^{42}K are from ref. ¹⁰⁾ and ref. ³¹⁾, respectively; spins and parities are from ref. ¹³⁾ and ref. ³²⁾, respectively.

Table 6 lists the coincidence relations obtained from the coincidence measurements.

In table 7 the γ -ray energies of strong background lines as calculated from the present investigation are compared to the values given by other authors.

Some rather strong γ -rays from the $^{39}\text{K}(n, \gamma)^{40}\text{K}$ reaction could not be positioned between levels known from the (d, p) work ¹⁰⁾. They were supposed to correspond to decay via other levels if both feeding and de-exciting γ -rays were observed (with energies checking within the experimental errors), and if the intensity balance was satisfactory. This has lead to four additional levels at $E_x = 2731, 3439, 4149$ and 4744 keV. These levels have also been reported in ref. ⁹⁾.

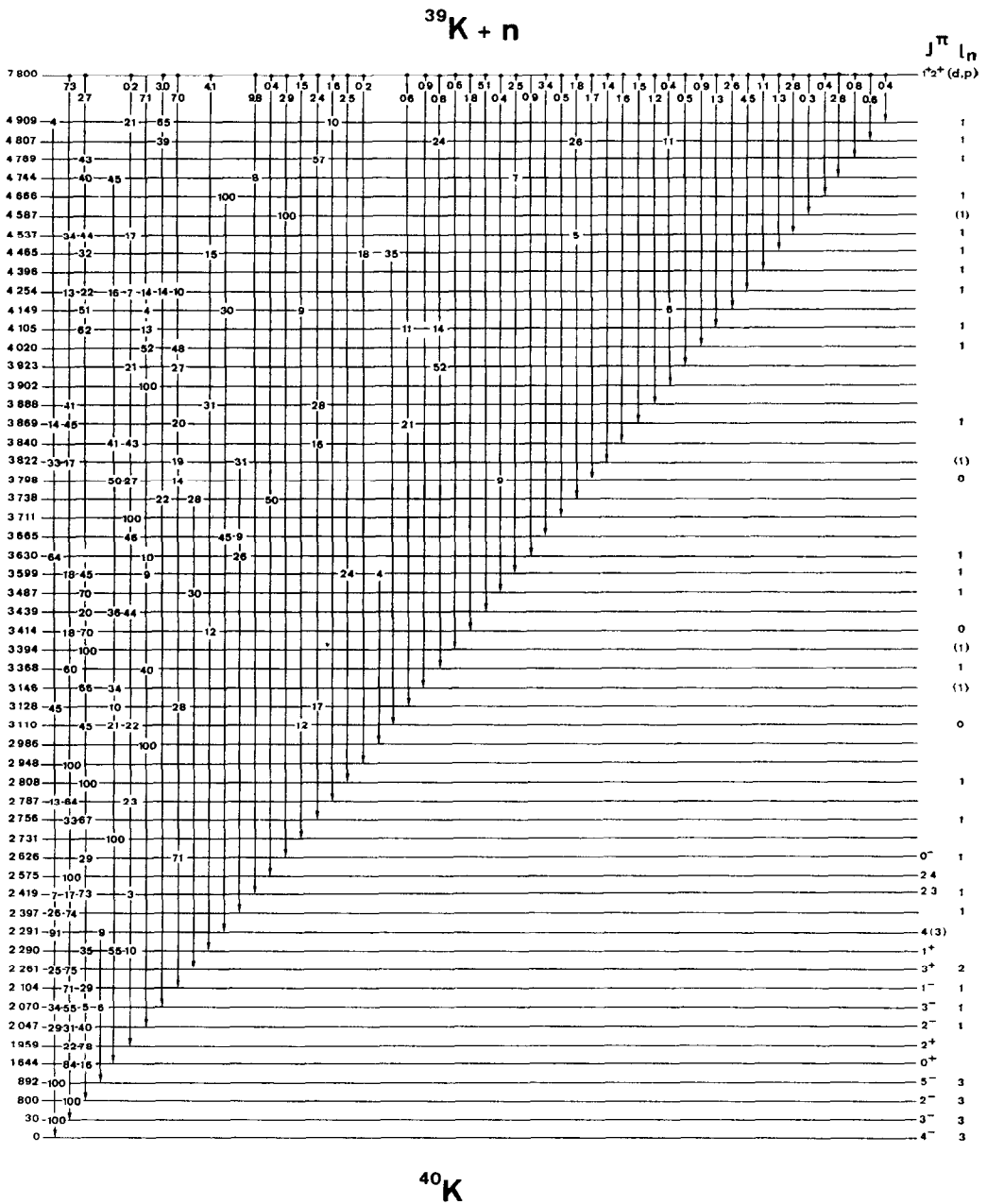
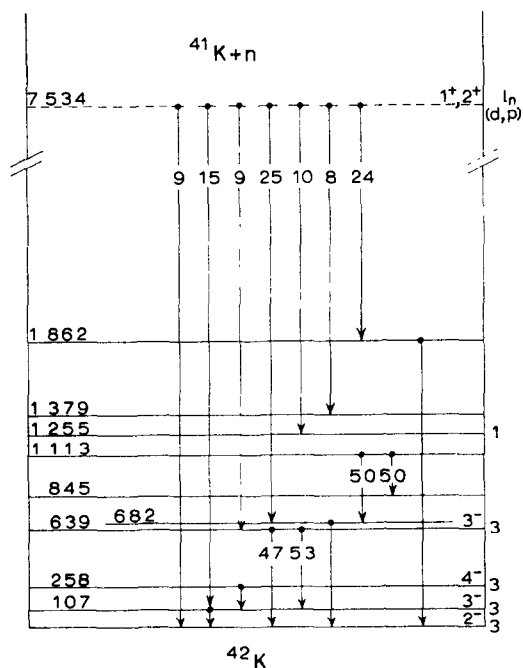


Fig. 3. Decay scheme of ^{40}K . The intensities of the primary γ -rays are normalized such that the sum equals 100. Branching ratios of the bound levels are given in percent.

Fig. 4. Decay scheme of ^{42}K .TABLE 5
Excitation energies of some levels in ^{42}K

E_x (keV) ^{a)}	E_x (keV) ^{a)}
107.1 ± 0.3	1113.3 ± 0.4
258.5 ± 0.3	1255.0 ± 0.6
639.0 ± 0.5	1378.7 ± 0.7
682.0 ± 0.3	1861.9 ± 0.5
844.9 ± 0.6	7533.9 ± 0.9 ^{b)}

^{a)} The results are obtained from a least-squares analysis (see text).^{b)} Reaction Q -value.TABLE 6
Results of γ - γ coincident measurements

Gate ^{a)} (E_γ in keV)	Coincident γ -rays (E_γ in keV)
6999	770
5752	770, 1247, 2018, 2048
5730	770, 1178, 1269, 2040, 2070
5696	770, 1303, 2074
5510	331, 646, 770, 1159, 1490, 1929
5381	770, 1159, 1619, 1929, 2389, 2419

^{a)} Windows placed on the corresponding double-escape peak in the Ge(Li) spectrum

TABLE 7
Energies of the strongest background γ -rays

$E_\gamma + E_r$ ^{a)} (keV)			Reaction
present work	other work	ref.	
110.1 \pm 0.2	109.8 \pm 0.2	¹⁸⁾	$^{19}\text{F}(\text{n}, \text{n}'\gamma)^{19}\text{F}$
197.2 \pm 0.3	197.2 \pm 0.2	¹⁸⁾	$^{19}\text{F}(\text{n}, \text{n}'\gamma)^{19}\text{F}$
583.5 \pm 0.3	583.5 \pm 0.2	¹⁸⁾	$^{19}\text{F}(\text{n}, \gamma)^{20}\text{F}$
656.1 \pm 0.3	656.3 \pm 0.3	¹⁸⁾	$^{19}\text{F}(\text{n}, \gamma)^{20}\text{F}$
	655.9 \pm 0.2	²⁶⁾	
983.4 \pm 0.4	983.8 \pm 0.3	¹⁸⁾	$^{19}\text{F}(\text{n}, \gamma)^{20}\text{F}$
	983.9 \pm 0.3	²⁶⁾	
1261.9 \pm 0.4	1261.76 \pm 0.07	¹⁸⁾	$^{12}\text{C}(\text{n}, \gamma)^{13}\text{C}$
	1261.92 \pm 0.06	²⁷⁾	
1293.6 \pm 0.3	1293.58 \pm 0.06	²⁸⁾	$^{40}\text{Ar}(\text{n}, \gamma)^{41}\text{Ar}(\beta^-)^{41}\text{K}$
1633.6 \pm 0.3	1633.7 \pm 0.3	¹⁸⁾	$^{19}\text{F}(\text{n}, \gamma)^{20}\text{F}(\beta^-)^{20}\text{Ne}$
1778.9 \pm 0.3	1778.70 \pm 0.17	²⁸⁾	$^{27}\text{Al}(\text{n}, \gamma)^{28}\text{Al}(\beta^-)^{28}\text{Si}$
	1779.1 \pm 0.3	²⁹⁾	$^{28}\text{Si}(\text{n}, \text{n}'\gamma)^{28}\text{Si}$
2223.3 \pm 0.2 ^{b)}	2223.35 \pm 0.05 ^{b)}	²¹⁾	$^1\text{H}(\text{n}, \gamma)^2\text{H}$
6129.6 \pm 0.8	6129.6 \pm 0.4	¹⁸⁾	$^{19}\text{F}(\text{n}, \alpha)^{16}\text{N}(\beta^-)^{16}\text{O}$
	6130.2 \pm 0.4	³⁰⁾	
7250.3 \pm 0.9	7250.0 \pm 1.0	²⁹⁾	$^6\text{Li}(\text{n}, \gamma)^7\text{Li}$
	7250.0 \pm 0.5	¹⁸⁾	
7278.2 \pm 1.0	7278.5 \pm 0.7	²⁹⁾	$^{56}\text{Fe}(\text{n}, \gamma)^{57}\text{Fe}$
7367.8 \pm 1.0	7367.5 \pm 0.7	²⁹⁾	$^{207}\text{Pb}(\text{n}, \gamma)^{208}\text{Pb}$
7631.1 \pm 1.0	7630.9 \pm 0.6	²⁹⁾	$^{56}\text{Fe}(\text{n}, \gamma)^{57}\text{Fe}$
7645.3 \pm 1.0	7645.3 \pm 0.6	²⁹⁾	$^{56}\text{Fe}(\text{n}, \gamma)^{57}\text{Fe}$

^{a)} The energy of the recoil correction is denoted by E_r .

^{b)} Uncorrected for recoil.

5. Discussion

Results from the present investigation are generally in agreement with those reported in refs. ^{9, 12, 13)}, though many differences occur especially with the results reported in ref. ⁹⁾, for the low-energy region. Some of the discrepancies are discussed below.

5.1. LEVELS NOT REPORTED IN REF. ⁹⁾

The $E_x = 2261$ keV level. The 2261 keV state de-excites by the 2231 and 2260 keV γ -rays. The first transition has not been reported in ref. ⁹⁾; the second is interpreted as a 2290 \rightarrow 30 keV transition. This interpretation has to be rejected because the 2260 keV γ -ray is not coincident with the 5510 keV γ -ray, which feeds the $E_x = 2290$ keV state. The present interpretation for the 2260 keV γ -ray, as a ground state transition, is based on intensities and is in agreement with the interpretation reported in ref. ¹³⁾.

The $E_x = 2290$ –2291 keV doublet. The computer program interprets the 2291 and 1399 keV γ -rays as de-exciting the 2290 keV level; the latter feeds the $E_x = 892$ keV

level. However, the two γ -rays are not observed in coincidence with the 5510 keV γ -ray feeding the $E_x = 2290$ keV level. Another position in the decay scheme is impossible for either γ -ray. This indicates a doublet at $E_x \approx 2290$ keV. The cascade γ -rays feeding the $E_x = 2291$ keV level have also been observed. The existence of the doublet is also suggested by Twin *et al.* ¹³⁾ on the basis of γ -ray angular distributions. The excitation energies are calculated as $E_x = 2289.8 \pm 0.3$ and 2290.5 ± 0.3 keV.

The $E_x = 2397$ keV level. The decay of the $E_x = 2397$ keV level has also been observed in the $^{40}\text{Ar}(p, n\gamma)^{40}\text{K}$ reaction ¹³⁾. The decay of this level is not reported in ref. ⁹⁾, although the 2367 keV γ -ray, which must be interpreted as a transition to the $E_x = 30$ keV level, was observed. Of the three γ -rays at $E_\gamma = 1233, 1266$ and 1424 keV feeding the $E_x = 2397$ keV level, only the first has been reported in ref. ⁹⁾.

The $E_x = 3923$ keV level. None of the γ -rays ($E_\gamma = 555, 1820$ and 1965 keV) de-exciting the $E_x = 3923$ keV level has been reported in ref. ⁹⁾. They appear clearly in the single spectrum (see fig. 1). The $E_\gamma = 3877.0 \pm 0.8$ keV γ -ray which feeds the $E_x = 3923$ keV level has been reported in ref. ⁹⁾ with slightly different energy: $E_\gamma = 3875.2 \pm 0.8$ keV.

The $E_x = 4666$ keV level. The 3133 and 2375 keV γ -rays feeding and de-exciting the $E_x = 4666$ keV level, respectively, have also been reported in ref. ⁹⁾. Another interpretation has been given because the $E_x = 2290$ keV level was not recognized as a doublet.

5.2. LEVELS REPORTED IN REF. ⁹⁾ BUT NOT FOUND IN THE PRESENT INVESTIGATION

The $E_x = 2458, 2558, 4273$ and 4281 keV levels. None of these levels has been reported [ref. ¹⁰⁾] from the (d, p) reaction. A 5341 keV γ -ray, $I_\gamma = 0.10 \pm 0.03$, reported ⁹⁾ to feed the $E_x = 2458$ keV level has not been observed in the present investigation. An upper limit for the intensity of this γ -ray should be $I_\gamma = 0.03$. The intensity balance for the reported $E_x = 2458$ keV level is poor: $I_{\text{in}}/I_{\text{out}} = 0.14 \pm 0.12$.

Two γ -rays, $E_\gamma = 1695$ and 2558 keV, feeding and de-exciting the $E_x = 2558$ keV level, respectively, have been reported in ref. ⁹⁾. The 1695 keV γ -ray should be interpreted as de-exciting the $E_x = 3797$ keV level. A peak at 2558 keV has not been observed ($I_\gamma \leq 0.06$) in the present investigation. The reported intensity of the 2558 keV γ -ray is $I_\gamma = 0.60 \pm 0.13$.

From the five γ -rays at $E_\gamma = 1646, 2629, 3382, 3473$ and 4254 keV, with $I_\gamma = 0.20 \pm 0.05, 0.40 \pm 0.10, 0.30 \pm 0.07, 0.20 \pm 0.05$ and 0.20 ± 0.05 , respectively, reported [ref. ⁹⁾] to de-excite the $E_x = 4273$ keV level, only one γ -ray ($3414 \rightarrow 30$ keV) has been observed in the present work ($I_\gamma = 0.42 \pm 0.10$). The upper limits for the intensities of the other γ -rays are 0.03, 0.08, 0.03 and 0.10, respectively. The reported γ -rays are transitions to levels with $J^\pi = 0^-, 0^+, 2^-, 3^-$ and 5^- . Consequently, whatever the J^π value of the 4273 keV level, one or more transitions should at least have octupole character, which also makes the given interpretation, and therefore the existence of the $E_x = 4273$ keV level, doubtful.

The 297 keV γ -ray, observed in the present investigation and which has been reported ⁹⁾ to feed the $E_x = 4281$ keV level must be ascribed to thermal-neutron capture in ^{72}Ge . The three γ -rays reported ⁹⁾ to de-excite this level have also been observed in the present experiment but the energies are such that they cannot originate from one level.

The $E_x = 3027$ and 3768 keV levels. Levels at $E_x = 3030 \pm 4$ and 3768 ± 4 keV are given in the review article of Endt and Van der Leun ¹¹⁾. From the three γ -rays which are reported ⁹⁾ to de-excite the $E_x = 3027$ keV level, the 609 keV γ -ray, also observed in the present investigation, must be ascribed to the $^{73}\text{Ge}(n, \gamma)^{74}\text{Ge}$ reaction, while the 973 and 2136 keV γ -rays with $I_\gamma = 0.10 \pm 0.03$ and 0.20 ± 0.05 , respectively, have not been observed in the present experiment ($I_\gamma \leq 0.01$ and ≤ 0.01 , respectively).

From the two γ -rays, which are reported ⁹⁾ to de-excite the $E_x = 3768$ keV level, the 1173 keV γ -ray must be ascribed to background radiation, while the peak at 3768 keV must be interpreted as the single-escape peak of the 4279 keV γ -ray.

5.3. THE DECAY OF SOME LOW-ENERGY LEVELS

The ground state transition of the first excited state is not observed in the present experiment because of the strong low-energy background radiation near the reactor. The excitation energy calculated from energy differences, $E_x = 29.8 \pm 0.2$ keV, is in reasonable agreement with the value reported in ref. ²⁵⁾ ($E_x = 29.52 \pm 0.10$ keV).

The decay of the $E_x = 800$ keV second excited state proceeds entirely via a 770 keV γ -ray to the $E_x = 30$ keV state. The $E_\gamma = 799.4 \pm 0.2$ keV γ -ray cannot be interpreted as a ground state transition of the $E_x = 800.1 \pm 0.2$ keV state as suggested by Johnson and Kennett ⁹⁾. This γ -ray has not been reported by Bass and Wechsung ²⁴⁾, Freeman and Gallman ¹²⁾ or Twin *et al.* ¹³⁾, which also indicates that this is a transition between two high-energy levels ($4537 \rightarrow 3738$ keV).

The branching ratios of the next five levels at $E_x = 892, 1644, 1959, 2047$ and 2070 keV are in good agreement with the results reported in refs. ^{9, 13)}. The decay of the $E_x = 2047$ and 2070 keV levels is confirmed by coincidence measurements (table 6).

A 2105 keV ground state transition ($I_\gamma = 0.80 \pm 0.15$) from the $E_x = 2104$ keV level as reported in ref. ⁹⁾ is less probable because (i) this transition is not reported in refs. ^{12, 13, 24)}, (ii) a 2104 keV γ -ray has not been observed in the present single spectrum ($I_\gamma \leq 0.06$), (iii) the present coincidence measurements which confirm the other decay branches from the 2104 keV state do not give any evidence for the existence of a 2104 keV γ -ray.

One of the γ -rays de-exciting the $E_x = 2419$ keV level, $E_\gamma = 459$ keV (feeding the $E_x = 1959$ keV level, has not been reported in ref. ¹³⁾. Alternatively it can be interpreted as a transition between the $E_x = 2104$ and 1644 keV levels. Observed coincidences between the 5381 keV γ -ray, which feeds the $E_x = 2419$ keV level, and the 1929 and 1159 keV γ -rays de-exciting the $E_x = 1959$ keV level make the interpretation

given here more probable. In the coincidence spectrum the 459 keV peak is obscured by the strong 511 keV annihilation peak.

The intensity of the γ -rays feeding the $E_x = 2575$ keV level is found to be too low (table 4). The decay of this level entirely proceeds by the 2546 keV γ -ray. This interpretation is supported by the $^{40}\text{Ar}(p, n\gamma)^{40}\text{K}$ data ¹³).

Different branchings have been found for the $E_x = 2626$ keV level. The present result is in good agreement with that reported in ref. ¹²).

5.4. SOME FINAL REMARKS ON THE $^{39}\text{K}(n, \gamma)^{40}\text{K}$ DECAY

Discrepancies exist with the results obtained by Johnson and Kennett ⁹) also for some high-energy levels (see table 4). These differences can mainly be explained by (i) different interpretations of the observed γ -rays in the decay scheme, (ii) differences in the energies of the observed γ -rays, (iii) differences in the interpretation of some peaks as full-energy, single- or double-escape peaks and (iv) a number of γ -rays which have been reported in ref. ⁹) as originating from the $^{39}\text{K}(n, \gamma)^{40}\text{K}$ reaction could be ascribed to background radiation or have not been observed in the present investigation. The intensities of these latter γ -rays are such that they would have been observed in the present investigation if they would originate from the $^{39}\text{K}(n, \gamma)^{40}\text{K}$ reaction. Some examples have been given in subsect. 5.2.

It was not possible to assign spins unambiguously on the basis of the present experiment, though for some levels spin restrictions may be possible.

5.5. REMARKS ON THE $^{41}\text{K}(n, \gamma)^{42}\text{K}$ DECAY

Energies and intensities of γ -rays from the $^{41}\text{K}(n, \gamma)^{42}\text{K}$ reaction have been reported by Skeppstedt ⁸) who used a sample enriched to 99.2 % in ^{41}K . Some γ -rays from the $^{41}\text{K}(n, \gamma)^{42}\text{K}$ reaction (investigated with a natural potassium target) have also been reported by Johnson and Kennett ⁹).

Three γ -rays at 433, 532 and 640 keV, reported ⁹) as originating from the $^{39}\text{K}(n, \gamma)^{40}\text{K}$ reaction must be ascribed to the $^{41}\text{K}(n, \gamma)^{42}\text{K}$ reaction, according to the present investigation. This interpretation is in agreement with that reported in ref. ⁸). The 532 and 640 keV γ -rays de-excite the $E_x = 639$ keV level; the first feeds the $E_x = 107$ keV level. A capture γ -ray at 6894 keV feeds the $E_x = 639$ keV level. This γ -ray has also been reported in ref. ⁸), but not in ref. ⁹).

By Johnson and Kennett ⁹) a 6915 keV capture γ -ray has been reported, leading to $E_x = 619$ keV, but γ -rays de-exciting this level have not been observed. In the present investigation this γ -ray has been observed, but could be ascribed to background radiation.

It is a pleasure to thank Professor P. M. Endt and Drs. C. van der Leun and H. Gruppelaar for their interest in this work. We like to thank V. Haase from the Kernforschungszentrum Karlsruhe for the Gauss-fit program and C. J. Zwakhals, T. van Ittersum and J. Akkermans for their help in the analysis of the spectra. This investi-

gation was performed as part of the research program of the Stichting voor Fundamenteel Onderzoek der Materie (FOM) with financial support from the Nederlandse Organisatie voor Zuiver Wetenschappelijk Onderzoek (ZWO).

References

- 1) T. H. Braid, *Phys. Rev.* **102** (1965) 1109
- 2) J. Urbanec, J. Kopecký and J. Kajfosz, *Czech. J. Phys.* **9** (1959) 544
- 3) B. B. Kinsey, G. A. Bartholomew and W. H. Walker, *Phys. Rev.* **85** (1952) 1012
- 4) G. A. Bartholomew and B. B. Kinsey, *Can. J. Phys.* **31** (1953) 927
- 5) B. P. Adyasevich *et al.*, *Atom. Energ.* **1** (1956) 28; *J. Nucl. Energ.* **3** (1956) 325
- 6) W. Rudolph and H. U. Gersch, *Nucl. Phys.* **71** (1965) 221
- 7) T. J. Kennett, L. B. Hughes and W. V. Prestwich, *Nucl. Phys.* **89** (1966) 254
- 8) O. Skeppstedt, *Proc. of the Int. Symp. on neutron capture gamma ray spectroscopy*, Studsvik, 1969, p. 217
- 9) L. V. Johnson and T. J. Kennett, *Can. J. Phys.* **48** (1970) 1109
- 10) H. A. Enge, E. J. Irwin and D. H. Weaner, *Phys. Rev.* **115** (1959) 949
- 11) P. M. Endt and C. van der Leun, *Nucl. Phys.* **A105** (1967) 1
- 12) R. M. Freeman and A. Gallmann, *Nucl. Phys.* **A156** (1970) 305
- 13) P. J. Twin, W. C. Olsen and D. M. Sheppard, *Nucl. Phys.* **A143** (1970) 481
- 14) G. A. Bartholomew *et al.*, *Nucl. Data* **A3** (1967) 367
- 15) G. van Middelkoop and P. Spilling, *Nucl. Phys.* **72** (1965) 1
- 16) P. Spilling, H. Gruppelaar and P. C. van den Berg, *Int. Symp. on Nucl. Electronics*, Versailles, 1968, Part II, Contr. 140
- 17) C. M. Lederer, J. M. Hollander and I. Perlman, *Table of isotopes*, 6th ed., appendix II (Wiley, New York, 1967)
- 18) P. Spilling, H. Gruppelaar, H. F. de Vries and A. M. J. Spits, *Nucl. Phys.* **A113** (1968) 395
- 19) R. L. Graham, *Nucl. Instr.* **9** (1960) 245
- 20) W. W. Black and R. L. Heath, *Nucl. Phys.* **A90** (1967) 650
- 21) H. W. Taylor, N. Neff and J. D. King, *Phys. Lett.* **24B** (1967) 659
- 22) J. H. E. Mattauch, W. Thiele and A. H. Wapstra, *Nucl. Phys.* **67** (1965) 32
- 23) H. Gruppelaar, A. M. F. Op den Kamp and A. M. J. Spits, *Nucl. Phys.* **A131** (1969) 180
- 24) R. Bass and R. Wechsung, *Phys. Lett.* **32B** (1970) 602
- 25) T. M. Young *et al.*, *Bull. Am. Phys. Soc.* **15** (1970) 1329
- 26) T. Holtebekk, S. Tryti and G. Vamraak, *Nucl. Phys.* **A134** (1969) 353
- 27) W. V. Prestwich, R. E. Coté and G. E. Thomas, *Phys. Rev.* **161** (1967) 1080
- 28) D. H. White and D. J. Groves, *Nucl. Phys.* **A91** (1967) 453
- 29) A. M. J. Spits, A. M. F. Op den Kamp and H. Gruppelaar, *Nucl. Phys.* **A145** (1970) 449
- 30) R. C. Greenwood, *Phys. Lett.* **23** (1966) 482
- 31) U. Lynen, H. Oeschler, R. Santo and R. Stock, *Nucl. Phys.* **A127** (1969) 343
- 32) W. H. Moore, J. W. Kelley and H. A. Enge, *MIT Lab. Nucl. Sci. Progr. Rept.* May 1958, p. 114